KYAU Journal, 5(2), 83-93

Khwaja Yunus Ali University Journal

Publisher homepage: www.kyau.edu.bd

OPEN ACCESS

ISSN: 2791-3759 (Online), 2521-3121 (Print)

Journal homepage: www.journal.kyau.edu.bd

Research Article

Comparison and Analysis of Pixel of Ultrasound B-images for Computer-aided Diagnosis by Using ImageJ Software

Bkash Chandra Roy[1], Abdus Sattar Mollah[1], M Matiur Rahman[1,*]

[1] Department of Medical Physics, Khwaja Yunus Ali University, Bangladesh

***Corresponding Author:** mrroyal2006@live.com (M Matiur Rahman, Assistant Professor & Head, Dept. of Medical Physics, Khwaja Yunus Ali University, Bangladesh)

Abstract

This study performed to ten various ultrasound images taken from the different ultrasound machines to detect the B mode image quality changing various parameters of ultrasound such as frequency, gain & dB. In addition, tissue thermal index (TIS) and mechanical index (MI) have been assessed. ImageJ software used to investigate different pixels and gray values by changing frequency, gain and dB and to acquire histogram, and graphical data, the GetData software was performed. In the case of gray value and pixel distance, some remarkable observations have been obtained by changing the frequency or gain or intensity (dB) and all data has been plotted. The pixel count of liver cirrhosis has been found higher than normal liver parenchyma however significant difference has been obtained for gallbladder stones than normal liver parenchyma. The tissue thermal index (TIS) and mechanical index (MI) were changed during scanning especially colour Doppler scanning depending on the selected area of interest, small selected area showed a higher tissue thermal index than the large selected area however mechanical index was the same.

Keyword: Ultrasound, Pixal Analysis, Diagnosis, ImageJ.

1. Introduction

Physics knowledge is needed in ultrasonic medical imaging, which is used a very high-frequency sound (> 20Khz) (Subedi *et al*., 2019). The attenuation of ultrasound by different body organs influences ultrasonic image formation. The ultrasonic power is related to the ultrasound beam intensity, and some related quantities (Labuda *et al*., 2022). The rate at which Energy passes through a unit cross-sectional area at a point in the propagating medium, and is measured in quantities like joules per second per square meter, is the relative scale, which is used to specify the intensity of an ultrasonic beam (Chen *et al*., 2015 & Pazinato *et al*., 2016). A suitable reference intensity is chosen on the relative scale, and all other intensities are then contrasted with it which is expressed as decibels (dB) (Lal *et al*., 2002 & Comeau *et al*., 2017). For instance, the decibel value 0dB may be considered as the reference intensity, which would be the output intensity of an ultrasonic device. As a result of attenuation, intensities at various tissue depths would have negative decibel values (Rangaraju *et al*., 2012).

There many record and display modes of ultrasound such as A-mode (1-dimentional), B-mode (2-dimentional), M-mode (to reveal moving structures), and so on. In any imaging system, image quality is a crucial factor. Instruments quality, particularly the transducer, beam frequency, and expert usage of the equipment affects the overall quality of the ultrasound image (Nguyen *et al.*, 2015). Various performance assessment and verification steps are involved in the development of an ultrasound imaging system. Understanding the connections between an ultrasound system's properties, such as the point spread function and pixel-based gray scale, and the system's clinical performance is necessary for evaluating the system's performance (Jeetendra Gochare *et al.*, 2016 & Kaur, 2013). The objectives of this study are (1) to acquire the Ultrasound B mode images of some body organs by using conventional Ultrasound machine, (2) to analyze the pixel gray scale of the images by using ImageJ software, (3) to perform the statistical analysis and (4) to determine bio-effect of ultrasonography based on physics of ultrasound.

2. MATERIALS AND METHOD

In this present study we used the following instruments and software:

2.1 Ultrasound Scanning Machines:

1. Philips: Clear view 350 with 2-5MHz curve linear probe.
2. Samsung Medison: R-5 with 2-5MHz curve linear probe were used to take B-mode Images of Liver, Kidney, pancreas, Gall bladder and Lung after appropriate consent.

These are the conventional ultrasound machines which are widely used to scan the different organs of the human body to detect various diseases such as functional abnormality, cancer, size measurement stone of gall bladder, kidney, urinary bladder etc. These are also randomly used to identify the fetal biophysical profile, congenital anomaly of pregnant mother.

2.2 ImageJ Software (32bit):

ImageJ is a java-based program created by the National Institutes of Health to process images. The open architecture of ImageJ allows for extension through Java plugins and recordable macros. ImageJ can edit, analyze, display, process, save, and print 8-bit color and grayscale, 16-bit integer, and 32-bit floating point images. Many raw image formats like JPG, GIF, JPEG, TIFF, BMP, PNG, and FITS are possible to read by it. Due to having multithreaded and multi-CPU hardware, a series of images can be processed by using this software. ImageJ can measure the user-defined pixel value statistics, intensity thresholded objects, distance and angles**.** A most exciting feature of it can show the line profile plots and density histograms automatically (Imagej Wiki., *2023*).

2.3 GetData (32bit):

When data values are missing, only scientific plots are available, GetData Graph Digitizer (Norman, *2013*) is a powerful tool to acquire the original data from the scanned (x,y) graph. In these situations, GetData Graph Digitizer makes it simple to obtain the numbers. Four steps make up the digitizing process:

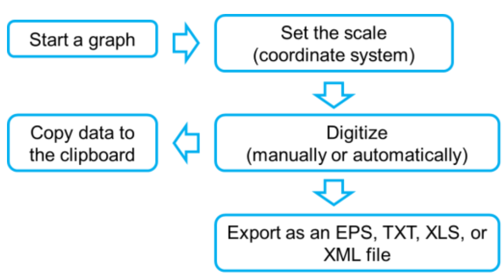

The following are GetData graph Digitizer's primary features:

- supported graphics formats are TIFF, JPEG, BMP and PCX;
- two algorithms for automatic digitizing;
- record tool for easy points recording;
- save /open workspace, which allows to save the work and return to it later;
- obtained data can be copied to the clipboard;
- export to the formats: TXT (text file), XLS (MS Excel), XML, DXF(AutoCAD), and EPS.

It is now possible to analyze B mode (brightness mode) images (10-images) with image analysis software image J (32bit) and Get data (32bit). Computers save grayscale images as a collection of distinct light spots, or pixels. Each pixel's brightness is represented by a value that goes from 0 for black to 80 for white. The same program is used to choose a specific area of interest in an image and calculate the median pixel brightness or intensity of that area.

2.4 Ultrasound Transmission Gel:

To reduce the tissue air gap during scanning by the US probe, gel was applied to the patient's skin surface at the area of interest for the coupling agent.

2.5 Equation of medical physics used:

1. $V_s \infty 1\sqrt{p}$ (v_s=velocity of sound, p= density, k= compressibility)
2. $V_s \infty 1\sqrt{k}$
3. $V_s = 1\sqrt{(kp)}$
4. dB(intensity)=10 $\log_{10}$(I/Io)

2.6 Used frequency, gain, decibel & mode of ultrasound and result of MI, TIS, gray value and pixel as Table 1.

Table 1: Used frequency, gain, decibel of ultrasound, mode and result of MI, TIS, gray value and pixel.

Frequency	Gain	Intensity (dB)	B-mode	Color Doppler	MI	TIS	Gray value of plot/graph		Pixel of	Histogram
							Minimum	Maximum	Mean	Maximum
21Hz	60	52	“	_	_	_	57	120	84.31	255
	60	52	“	_	_	_	42	61	41.99	255
	80	51	“	_	_	_	60	122	86.42	255
24Hz	80	58	“	_	_	_	82	95	79.72	248
	60	58	“	_	_	_	65	72	55.96	189
	66	58	“	_	_	_	72	102	78.92	208
29Hz	60	52	“	_	_	_	38	85	65.89	190
	60	52	“	_	_	_	50	59	47.8	189
	80	51	“	_	_	_	_	_	_	_
30Hz	41	52	“	_	_	_	47	67	59.34	119
	41	52	“				97	122	113.9	178
	41	52	“	_	_	_	59	60	47.82	102
	41	52	“				68	70	65.52	103
33Hz	66	58	“	_	_	_	68	88	69.23	213
	60	52	“				34,44	72,52	57,60	193,189
	55	52	“	_	_	_	5, 46	64,70	32,60	255,158
2.5MHz	50	51	“	√	1.0	0.4	_	_	_	_
	50	51	“	√	1.0	0.6	_	_	_	_
	50	51	“	√	1.0	0.6	_	_	_	_
	50	51	“	√	1.0	0.7	_	_	_	_

2.7 Image of ultrasound machine & gel:

(a) (b) (c)

Fig. 1: (a) Philips Clear view 350 ultrasound machine, (b) Samsung Medison R-5 ultrasound machine, and (c) Ultrasound transmission Gel used to minimize the tissue air gap during taking the images.
These are used to take the images of different abdominal organs of human body.

3. Results and Discussion

Using a standard US machine, a number of B-mode pictures of various body organs have been taken to analyze. The analysis of the results is given in the following section.

3.1 Image Analysis of Kidney:

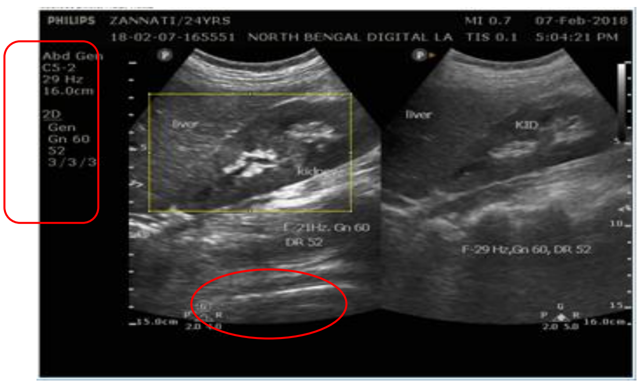

Fig.2 (a): US image of kidney.

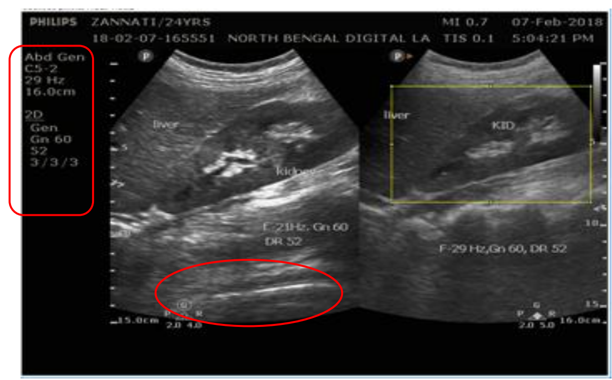

Fig. 2 (b): US image of kidney.

These images of kidneys (Fig. 2) are taken using frequency of 21Hz (Lt. sided selected area of kidney image) and 29Hz (Rt. sided same selected area of kidney image) however gain is same i.e. 60 and power 52. These two images are showing different pixel and gray value when analyzed by using imageJ software as shown in below histogram and plot (Imagej Wiki., *2023*).

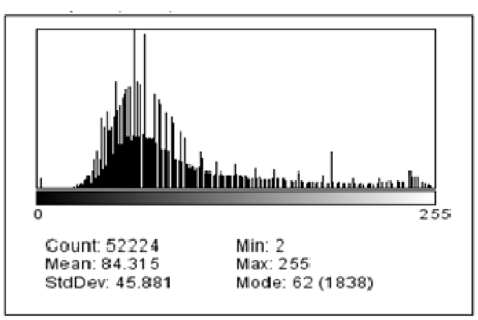

Fig. 2.1(a) Pixels histogram of kidney.

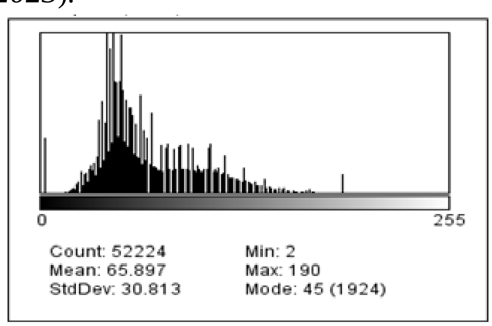

Fig. 2.1(b) Pixels histogram of kidney.

Above histogram for frequency of 21Hz shows mean pixel count is 84.31, In contrast, the mean count is 65.89, the standard deviation is 30.91, and the maximum count is 190 with a frequency of 29 Hz. These histograms indicate that 21Hz frequency is better than 29Hz for getting higher pixel value using same gain. These are happened due to higher frequency less depth of penetration due to more attenuation and lower frequency greater depth of penetration due to less attenuation**.** The below plot analysis of two images are showing that the gray value is higher for 21Hz frequency than 29Hz i.e. peak gray value is 120 corresponding 200 pixel for 21Hz whereas about 85 gray value corresponding 200 pixel for 29Hz. So, we can say that ultrasound image quality is frequency dependent and the frequency is depth and density dependent because human kidneys are deeper organs thus not so high or not so low, optimum frequency is needed for optimum penetration and better resolution.

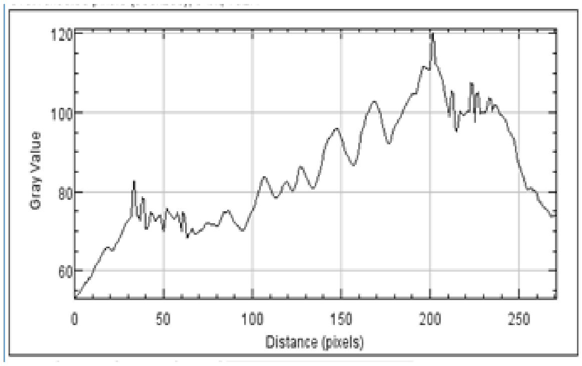

Fig. 2.2(a) Graph of gray value & pixels of kidney.

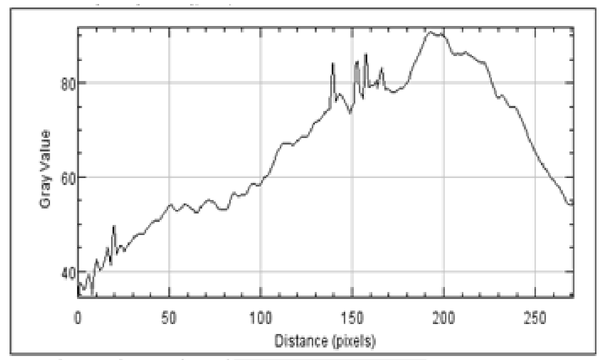

Fig. 2.2(b) Graph of gray value & pixels of kidney

3.2 Image analysis of Liver:

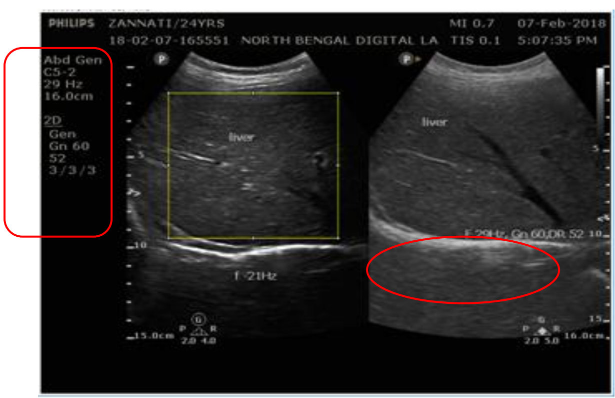

Fig. 3 (a): US image of Liver.

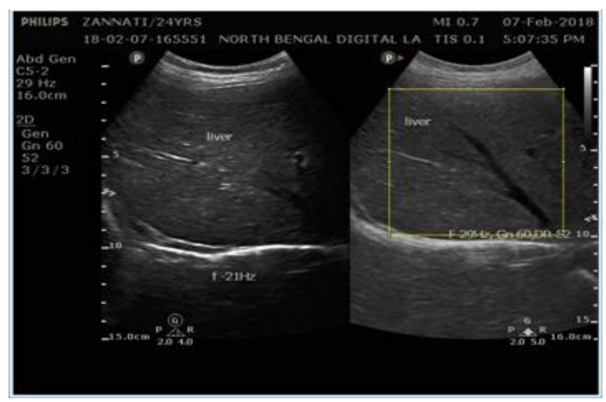

Fig. 3 (b): US image of Liver.

The images of liver (Fig. 3) are taken using frequency of 21Hz (Lt. sided selected area of liver image) and 29Hz (Rt. Sided same selected area of liver image) however gain is same i.e., 60 (as shown in image). These two images are showing different pixel and gray value when analyzed by using image J software as shown in below histogram and plot.

Below histogram for frequency of 21Hz shows mean pixel count is 41.99, Std. Dev. is 22.11 and maximum count is 255 whereas mean count is 47.80, Std. Dev. is 19.05 and maximum count is 189 for the frequency of 29Hz. These histograms indicate that 21Hz frequency provides higher pixel than 29Hz using same gain. These are happened due to theory of higher frequency more attenuation so less depth penetration like that lower frequency less attenuation and greater depth of penetration in a given distance (Zagzebski, *1996*).

.

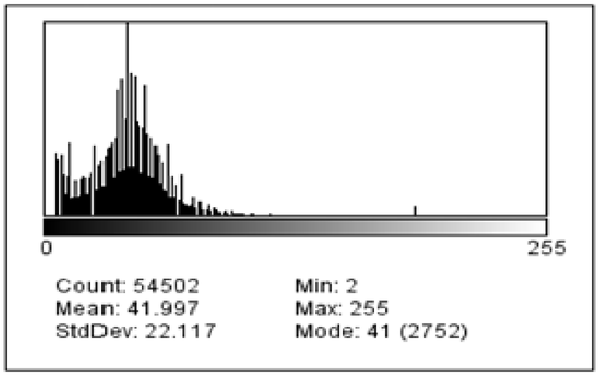

Fig. 3.1(a) Pixels histogram of liver.

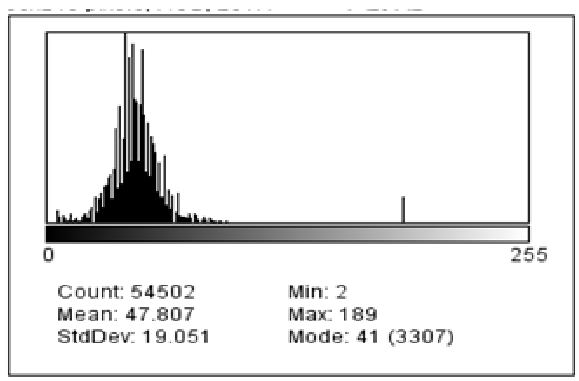

Fig. 3.1(b) Pixels histogram of liver.

The below plot analysis of two images are showing that the gray value is higher for 21Hz frequency than 29Hz i.e., peak gray value is more than 60 regarding 90 pixel for 21Hz whereas less than 60 regarding 25pixel for 29Hz. These plots indicate that ultrasound image quality is frequency dependent and the frequency is depth and density dependent because human liver is deeper organ thus optimum frequency for optimum depth is needed for better image.

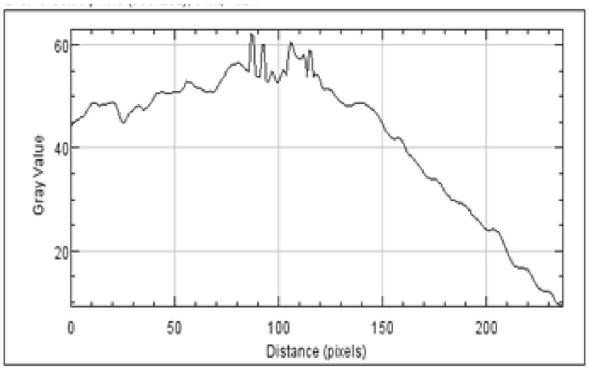

Fig. 3.2(a) Graph of gray value & pixels of liver.

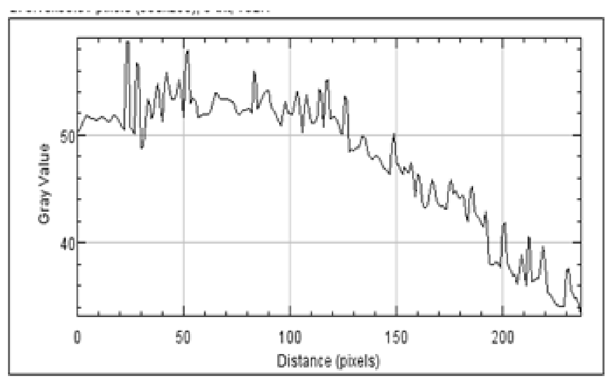

Fig. 3.2(b) Graph of gray value & pixels of liver.

3.3 Image analysis of Liver and Gall bladder:

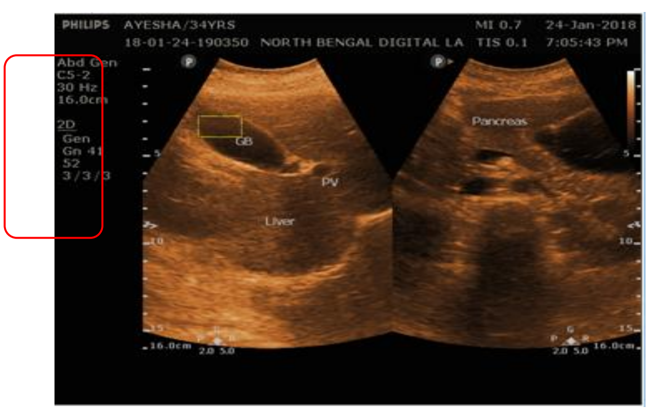

Fig. 4 (a) US image of Gall bladder.

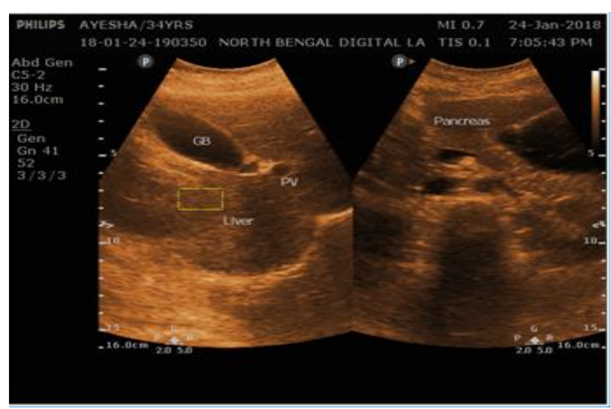

Fig.4 (b) US image of Liver.

These images are taken using same frequency of 30Hz, same gain of 41and power 52. These two images Lt. sided selected area of gall bladder image and Rt. sided selected same area of liver image are showing different pixel and gray value when analyzed by using imageJ software as shown in below histogram and plot.

Below histogram for selected area of gall bladder showing mean pixel count is 47.82, Std. Dev. is 9.85and maximum count is 102 whereas mean count is 65.52, Std. Dev. is 8.37 and maximum count is 103 for liver image of selected area. These two histograms indicate that mean count of pixel for liver is higher than gall bladder. These are happened due to sound traveling at higher speeds through gall bladder because it is fluid filled so that through transmission of sound occur on the other hand higher density more attenuation (the combined effect of scattering and absorption/decay rate as it propagates through medium) less penetration in a given distance (Zagzebski, *1996*).

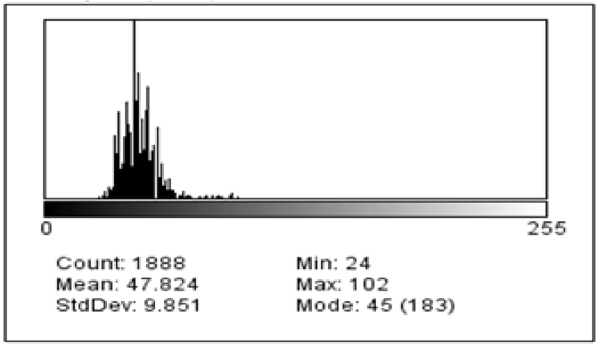

Fig. 4.1(a) Pixels histogram of gall bladder.

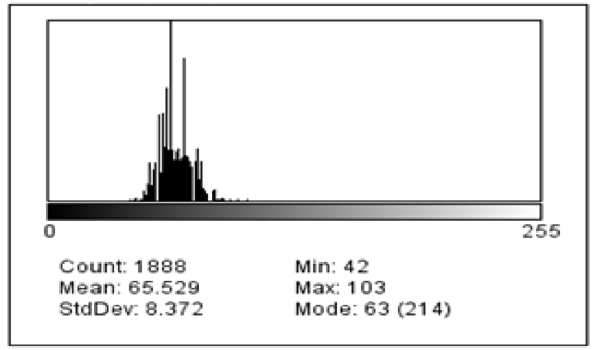

Fig. 4.1(b) Pixels histogram of liver.

The below plot analysis of two images are showing that the gray value is higher for liver than Gall bladder using same frequency 30Hz. In case of liver tissue gray value is starting from 68 and reached at 70 for 50 pixels whereas in case of gall bladder gray value is starting from 60 and reached at 49 for 50 pixels. These plots indicate that B mode ultrasound gray value is density dependent because human liver is denser than gall bladder lumen containing bile/liquid (Curry *et. al., 1995*).

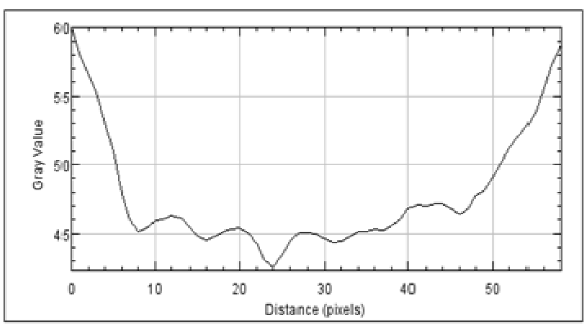

Fig. 4.2(a) Graph of gray value & pixels of gall bladder.

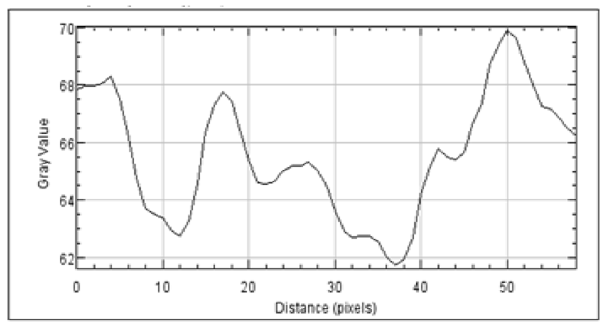

Fig. 4.2(b) Graph of gray value & pixels of liver.

3.4 Image analysis of Liver & lung:

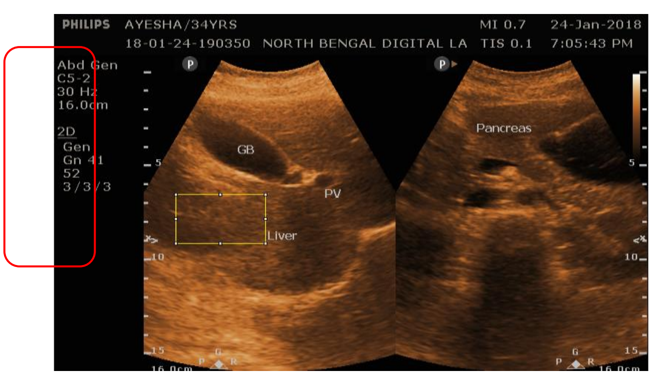

Fig. 5 (a) US image of liver.

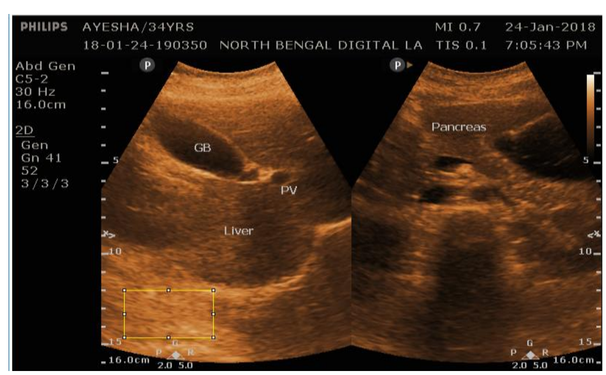

Fig. 5(b). US image of Lung.

These images of liver and lung are taken using same frequency of 30Hz, same gain of 41and power 52. These two images Lt. sided selected area of liver parenchyma and Rt. sided selected same area of lung parenchyma are showing different pixel and gray value when analyzed by using imageJ software as shown in below histogram and plot**.**

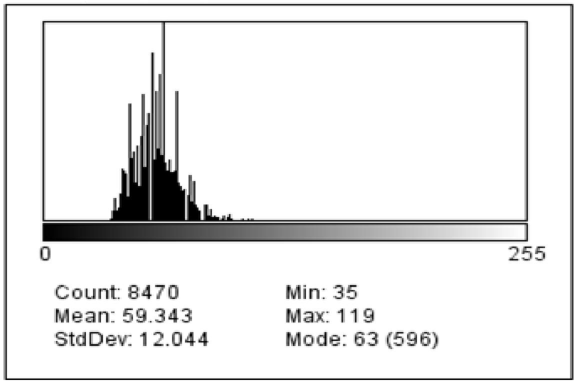

Fig.5.1(a) Pixels histogram of liver.

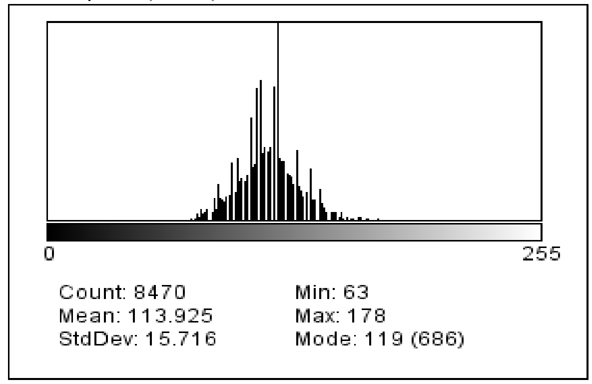

Fig.5. 1(b) Pixels histogram of lung.

Above histogram for selected area of liver parenchyma showing mean pixel count is 59.34, Std. Dev. is 12.04 and maximum count is 119 whereas mean count is 113.92, Std. Dev. is 15.71 and maximum count is 178 for lung parenchyma of same selected area. These two histograms indicate that mean pixel count for lung parenchyma is much higher than liver parenchyma because of lungs containing air where there is more attenuation occur (absorption and scattering) so that more reflection of sound occur than liver.

The below graph analysis of two images are representing that the gray value is higher for lung than liver using same frequency 30Hz. In case of liver tissue peak gray value is 68 for 62 pixels whereas in case of lung peak gray value is 125 for 90 pixels. These graphs indicate that B mode ultrasound gray value and pixel depend on medium where there is different level of sound attenuation occur during propagation (Yeh *et a1., 2003*).

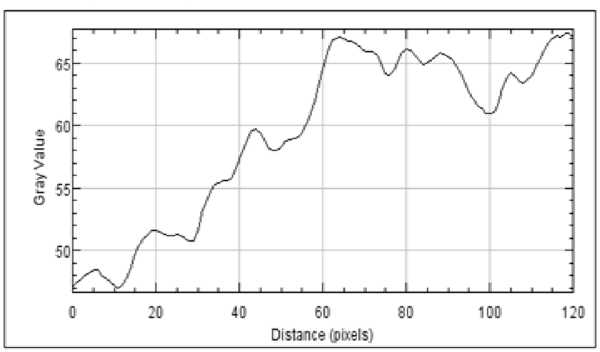

Fig.5.2(a) Graph of gray value & pixels of liver.

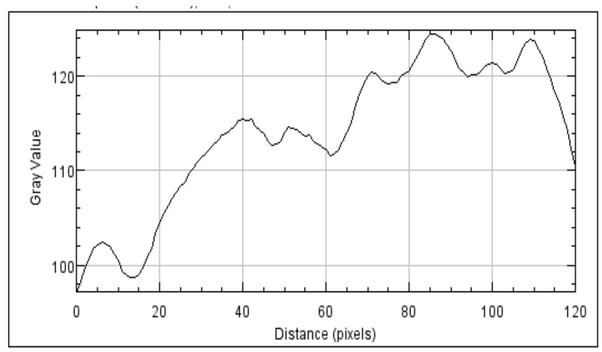

Fig.5.2(b) Graph of gray value & pixels of lung.

3.5 Image analysis of Kidney (Color Doppler):

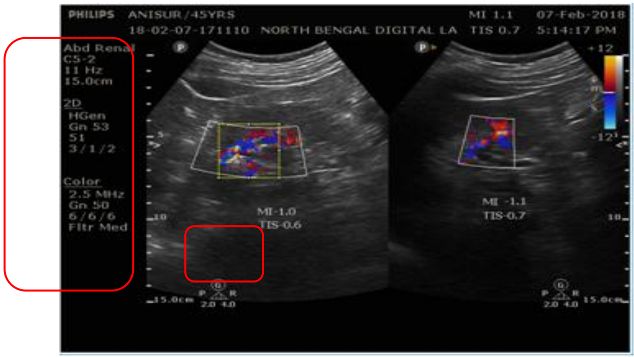

Fig. 6 (a): US image of Kidney.

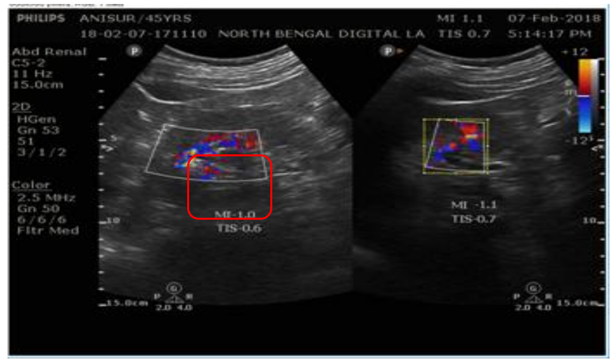

Fig. 6 (b): US image of Kidney.

These images of human liver are taken firstly using same frequency of 11Hz and same gain of 53 for B mode ultrasonography then 2.5MHz and gain 50 for color Doppler ultrasonography as shown in white box in images. Lt. sided selected area is larger than Rt. (white color box of images), Lt. side representing mechanical index (MI) 1.0 and soft tissue thermal index (TIS) 0.6 for large selected area (Lt. sided yellow box of image) however Rt. side representing MI 0.7 and TIS 1.1 for small selected area (Rt. sided yellow box of image).

These findings showed that the thermal effect for color Doppler depends on the biological tissue's selected area, i.e., less selected areas during scanning produce more thermal effect, and vice versa. This is because the same sound energy is transmitted to and absorbed by both large and small areas of biological tissue, which is then converted to heat energy, so that small area generates higher TIS than large area. When these two images are analyzed by imageJ software different pixel and gray values are found as shown in below histogram and plot/graph**.**

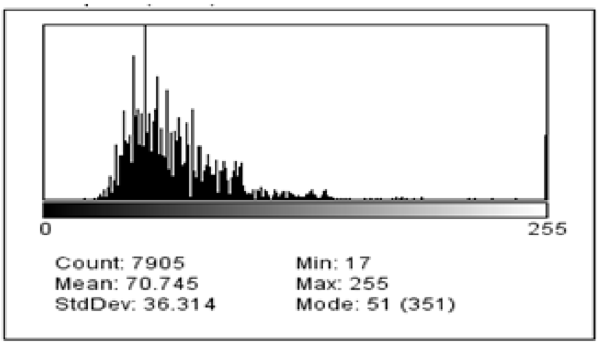

Fig.6.1(a) Pixels histogram of kidney.

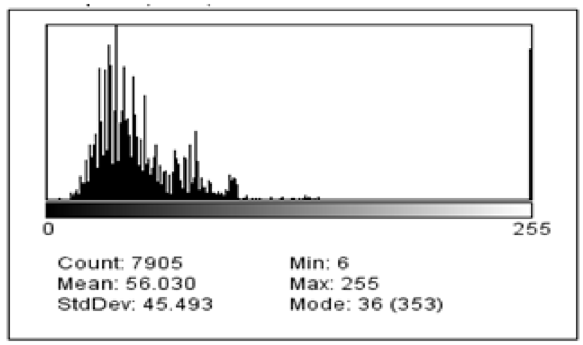

Fig.6.1(b) Pixels histogram of kidney.

The histogram for selected area of Lt. liver parenchyma showing mean pixel count is 70.74, Std. Dev. is 36.31and maximum count is 255 whereas mean count is 56.03, Std. Dev. is 45.49 and maximum count is 255 for same selected area Rt.

These two histograms indicate that mean pixel count for large selected area of liver parenchyma of Doppler scanning is higher than small selected area of liver parenchyma (Rt. image).

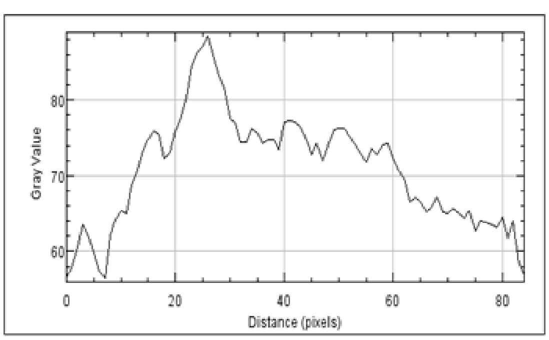

Fig.6.2(a) Graph of gray value & pixels of kidney.

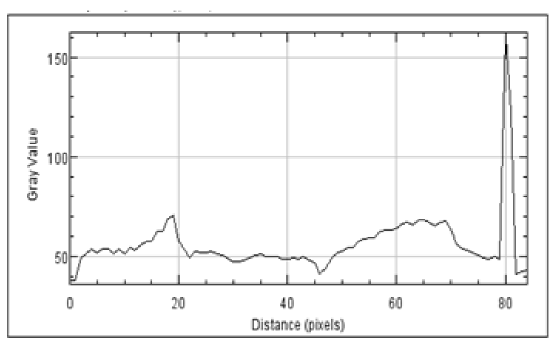

Fig.6.2(b) Graph of gray value & pixels of kidney.

4. Conclusion

In case of soft tissue changing the frequency, remaining same gain and intensity (dB) higher gray value and pixel distance has been found for comparatively low frequency than high due to more attenuation of sound energy (histogram 3.1a & b and graph no. 3.2a & b) conversely in incase of fluid medium sound energy travel faster than soft tissue due to less attenuation thus produce anechoic area (dark area) and posterior acoustic enhancement (brightness) due to comparatively more attenuation of sound than fluid (image no 3, histogram and plot no. 3.a& b). Likewise changing the gain remaining same frequency and dB higher gray value and pixel has been obtained for comparatively higher gain than low gain. However, changing dB remaining same frequency and gain reverse result has been obtained i.e., higher gray and pixel distance has been found comparatively low dB than high. In addition, tissue thermal index (TIS) and mechanical index (MI) has been observed in different analysis and all the results were below the normal range of biological effect (Table 1). In this way, it has been tried to prove that US image and pixel is frequency, dB (intensity) and gain dependent and these parameters are tissue density dependent (Table 1).

These characteristics, and continued improvements in image quality and resolution have expanded the use of US to many areas in medicine beyond traditional diagnostic imaging applications such as interventional procedures. The understanding of these basic physical principles can help to improve the image quality as well as diagnosis of diseases.

5. Acknowledgement

We are very much grateful to North Bengal Digital Diagnostic Center and Suraiya Diagnostic Center, Gaibandha for their permission and instrumental support to fulfill this research work.

6. Authors Contributions

All types of materials, data collection, analysis, graphical representation, manuscript typing, and formatting for this study were prepared jointly by Bkash Chandra Roy and Md. Matiur Rahman. This study is supervised by Prof. Dr. Abdus Sattar Mollah, who also made all types of corrections and finalized the document.

7. Funding

This study did not receive any specific grants from public, commercial, or non-profit funding bodies.

8. Disclosure

The authors declared no prospective conflicts of interest with respect to the research.

5. References

1. Chen, J., You, H., & Li, K. (2020). A review of thyroid gland segmentation and thyroid nodule segmentation methods for medical ultrasound images. *Computer methods and programs in biomedicine*, *185*, 105329. https://doi.org/10.1016/j.cmpb.2020.105329

2. Comeau, E. S., Hocking, D. C., & Dalecki, D. (2017). Ultrasound patterning technologies for studying vascular morphogenesis in 3D. *Journal of cell science*, *130*(1), 232-242. https://doi.org/10.1242/jcs.188151.

3. Curry, R. A., & Tempkin, B. B. (1995). *Ultrasonography: an introduction to normal structure and functional anatomy*. Saunders.

4. Imagej Wiki. (n.d.). Retrieved January 31, 2023, from https://imagej.net/

5. Jeetendra Gochare, P. C. (2016). Pixel Measurement of thyroid Gland by Using Ultrasound Image. International Journal of Engineering Science & Research Technology, 5(7), 883–888. https://doi.org/10.5281/zenodo.57945.

6. Kaur, K. (2013). Digital image processing in ultrasound images. *International Journal on Recent and Innovation Trends in Computing and Communication*, *1*(4), 388-393.

7. Labuda, C., Newman, W. R., Hoffmeister, B. K., & Chambliss, C. K. (2022). Two-dimensional mapping of the ultrasonic attenuation and speed of sound in brain. *Ultrasonics*, *124*, 106742.

8. Lal, B. K., Hobson II, R. W., Pappas, P. J., Kubicka, R., Hameed, M., Chakhtura, E. Y., ... & Durán, W. N. (2002). Pixel distribution analysis of B-mode ultrasound scan images predicts histologic features of atherosclerotic carotid plaques. *Journal of vascular surgery*, *35*(6), 1210-1217.

https://doi.org/10.1067/mva.2002.122888

9. Nguyen, N. Q., & Prager, R. W. (2015). High-resolution ultrasound imaging with unified pixel-based beamforming. *IEEE transactions on medical imaging, 35*(1), 98-108.
10. Norman, G. (2014, January 8). *» Download GetData Graph Digitizer Free*. Retrieved January 31, 2023, from http://getdata-graph-digitizer.findmysoft.com/
11. Pazinato, D. V., Stein, B. V., de Almeida, W. R., Werneck, R. D. O., Júnior, P. R. M., Penatti, O. A., ... & Rocha, A. (2014). Pixel-level tissue classification for ultrasound images. *IEEE journal of biomedical and health informatics*, *20*(1), 256-267.
12. Rangaraju, D. K. S., Kumar, K., & Renumadhavi, C. (2012). Review paper on quantitative image quality assessment–medical ultrasound images. *Int. J. Eng. Research and Technology*, *1*(4).
13. Subedi, Aabiskar. (2019). Ultrasound and It's Application on Medicine (Ultrasonography): A Term Paper. 10.13140/RG.2.2.10777.24161.
14. Yeh, W. C., Huang, S. W., & Li, P. C. (2003). Liver fibrosis grade classification with B-mode ultrasound. Ultrasound in medicine & biology, 29(9), 1229–1235. https://doi.org/10.1016/s0301-5629(03)01010-x.
15. Zagzebski J. A. (1996). *Essentials of ultrasound physics*. Mosby.

Citation: Roy,B.K, Mollah,A.S., & Rahman,M.M. (2022). Comparison and Analysis of Pixel of Ultrasound B-images for Computer-aided Diagnosis by Using ImageJ Software. *Khwaja Yunus Ali Uni.J*, 5(2),83-93